Biochimica et Biophysica Acta 1843 (2014) 902–914

Contents lists available at ScienceDirect

Biochimica et Biophysica Acta

journal homepage: www.elsevier.com/locate/bbamcr

The anti-fibrotic effects of CCN1/CYR61 in primary portal myofibroblasts are mediated through induction of reactive oxygen species resulting in cellular senescence, apoptosis and attenuated TGF-β signaling

Erawan Borkham-Kamphorst [a,*], Christian Schaffrath [a], Eddy Van de Leur [a], Ute Haas [a], Lidia Tihaa [a], Steffen K. Meurer [a], Yulia A. Nevzorova [b], Christian Liedtke [b], Ralf Weiskirchen [a,*]

[a] Institute of Clinical Chemistry and Pathobiochemistry, RWTH Aachen University Hospital, Germany
[b] Department of Internal Medicine III, RWTH Aachen University Hospital, Germany

ARTICLE INFO

Article history:
Received 11 October 2013
Received in revised form 28 December 2013
Accepted 21 January 2014
Available online 31 January 2014

Keywords:
Portal myofibroblast
Hepatic stellate cell
Myofibroblast
Apoptosis
CCN protein
Senescence

ABSTRACT

Cysteine-rich protein 61 (CCN1/CYR61) is a CCN (CYR61, CTGF (connective tissue growth factor), and NOV (Nephroblastoma overexpressed gene)) family matricellular protein comprising six secreted CCN proteins in mammals. CCN1/CYR61 expression is associated with inflammation and injury repair. Recent studies show that CCN1/CYR61 limits fibrosis in models of cutaneous wound healing by inducing cellular senescence in myofibroblasts of the granulation tissue which thereby transforms into an extracellular matrix-degrading phenotype. We here investigate CCN1/CYR61 expression in primary profibrogenic liver cells (*i.e.*, hepatic stellate cells and periportal myofibroblasts) and found an increase of CCN1/CYR61 expression during early activation of hepatic stellate cells that declines in fully transdifferentiated myofibroblasts. By contrast, CCN1/CYR61 levels found in primary parenchymal liver cells (*i.e.*, hepatocytes) were relatively low compared to the levels exhibited in hepatic stellate cells and portal myofibroblasts. In models of ongoing liver fibrogenesis, elevated levels of CCN1/CYR61 were particularly noticed during early periods of insult, while expression declined during prolonged phases of fibrogenesis. We generated an adenovirus type 5 encoding CCN1/CYR61 (*i.e.*, Ad5-CMV-CCN1/CYR61) and overexpressed CCN1/CYR61 in primary portal myofibroblasts. Interestingly, overexpressed CCN1/CYR61 significantly inhibited production of collagen type I at both mRNA and protein levels as evidenced by quantitative real-time polymerase chain reaction, Western blot and immunocytochemistry. CCN1/CYR61 further induces production of reactive oxygen species (ROS) leading to dose-dependent cellular senescence and apoptosis. Additionally, we demonstrate that CCN1/CYR61 attenuates TGF-β signaling by scavenging TGF-β thereby mitigating *in vivo* liver fibrogenesis in a bile duct ligation model. *Conclusion*: In line with dermal fibrosis and scar formation, CCN1/CYR61 is involved in liver injury repair and tissue remodeling. CCN1/CYR61 gene transfer into extracellular matrix-producing liver cells is therefore potentially beneficial in liver fibrotic therapy.

1. Introduction

Cysteine-rich protein 61 (CCN1/CYR61) is a CCN family matricellular protein comprising six secreted CCN proteins in mammals. The CCN acronym is derived from the first three identified members of this family, CYR61, CTGF (connective tissue growth factor), and NOV (Nephroblastoma overexpressed gene) [1,2]. CCN1/CYR61 is an important regulator of inflammation and wound repair. It is strongly expressed in myofibroblasts (MFB) of granulation tissue and controls fibrosis through cellular senescence. MFB are recruited in cutaneous wound healing to form the granulation tissue where they proliferate and rapidly synthesize extracellular matrix (ECM) components to provide tissue integrity during repair. At later stages of wound healing, MFB are driven into senescence by CCN1/CYR61, whereupon they transform into an ECM-degrading phenotype, thus limiting fibrosis [1,3]. Effectively, CCN1/CYR61 functions as an anti-fibrotic molecular switch that converts ECM-producing MFB into ECM-degrading senescent cells [4,6].

The CCN1/CYR61-induced senescence switch occurs at later stages of wound healing, exerting a self-limiting effect on the synthesis and deposition of ECM by MFB in several ways. First, senescent MFB no longer proliferate, thereby curbing the number of ECM-producing cells. Second, senescent cells express the anti-fibrotic senescence-associated

Abbreviations: α-SMA, α-smooth muscle actin; BDL, bile duct ligation; β-Gal, β-galactosidase; CCN1/CYR61, cysteine-rich protein 61; ECM, extracellular matrix; HSC, hepatic stellate cell(s); LCN2, lipocalin 2; MFB, myofibroblast(s); PDGF-BB, platelet-derived growth factor-BB; PDGFRβ, platelet-derived growth factor receptor type β; pMF, portal myofibroblast(s); ROS, reactive oxygen species; TGF-β1, transforming growth factor-β1; TUNEL, terminal transferase dUTP nick end-labeling; qRT-PCR, quantitative real-time PCR

* Corresponding authors at: Institute of Clinical Chemistry and Pathobiochemistry, RWTH-University Hospital, D-52074 Aachen, Germany. Tel.: +49 241 8088683; fax: +49 241 8082512.
E-mail addresses: ekamphorst@ukaachen.de (E. Borkham-Kamphorst), rweiskirchen@ukaachen.de (R. Weiskirchen).

0167-4889/$ – see front matter © 2014 Elsevier B.V. All rights reserved.
http://dx.doi.org/10.1016/j.bbamcr.2014.01.023

secretory phenotype resulting in increased expression of matrix metalloproteinases and reduced expression of collagen, leading to matrix degradation. Third, senescent cells are cleared by natural killer cells, thus accelerating wound resolution. Hence, CCN1/CYR61 turns the ECM synthesizing MFB themselves into ECM-degrading senescent cells, thereby imposing a self-limiting effect on fibrogenesis and promoting wound resolution [4,6].

Knock-in mice expressing a CCN1/CYR61 mutant that is unable to bind the α6β1-heparan sulfate proteoglycans are defective for senescence induction [7]. Consequently, senescent cells do not accumulate in the granulation tissue during wound healing, resulting in exacerbated fibrosis. Topical application of purified recombinant CCN1/CYR61 protein to cutaneous wounds however does reverse these defects, further underlining the critical role of CCN1/CYR61 in controlling MFB senescence to limit fibrosis [5].

Liver fibrosis results from wound-healing responses characterized by the accumulation of ECM following injury [8,9]. If the insult is acute or self-limited, the liver architecture restores to its normal composition, but if the injury is sustained, chronic inflammation and accumulation of ECM will persist and lead to progressive substitution of liver parenchyma through scar tissue formation.

Recent studies showed senescent hepatic stellate cells (HSC) to accumulate in carbon tetrachloride (CCl_4)-induced liver damage and dampen liver fibrosis through expression of anti-fibrotic proteins, suggesting that senescent cells may arise to limit fibrosis during tissue repair, but this phenomenon has not yet been examined beyond CCl_4-induced liver injury. In mice lacking key senescence regulators, HSC continue to proliferate, leading to excessive liver fibrosis and scar formation [10].

In addition to cutaneous wound healing, CCN1/CYR61 expression is elevated in remodeling cardiomyocytes after myocardial infarctions [11], during vascular injury [12], and in the long bones during fracture repair, specifically in proliferating chondrocytes and osteoblasts [13]. In line, it was demonstrated that CCN1/CYR61 blockage by antibodies inhibits bone fracture healing in mice [14]. In kidney, this CCN protein is expressed in podocytes in normal adult and embryonic glomeruli, but CCN1/CYR61 expression is strongly decreased in IgA nephropathy, diabetic nephropathy and membranous nephropathy, particularly in diseased kidneys with severe mesangial expansion [15]. CCN1/CYR61 impaired functioning therefore may contribute to the progression of glomerular disease with mesangial expansion. The precise role of CCN1/CYR61 in liver fibrogenesis still requires further research.

We here investigate CCN1/CYR61 gene expression in different primary liver cells, and liver tissue from animals undergoing bile duct ligation (BDL) and CCl_4 treatment, using quantitative real-time PCR (qRT-PCR), Western blotting, and immunohistochemistry to query the effects of CCN1/CYR61. CCN1/CYR61 protein was further overexpressed in cirrhotic fat storing cell lines CFSC, portal myofibroblasts (pMF) and HSC, using plasmid transfection and adenoviral gene expression. We showed CCN1/CYR61 to induce cellular apoptosis in CFSC, pMF and HSC and reduce expression of fibrotic markers, including collagen type I α1 (col1α1) and α-smooth muscle actin (α-SMA). CCN1/CYR61 induces apoptosis through induction of reactive oxygen species (ROS) as confirmed by elevated levels of cleaved caspase, caspase activity and terminal transferase dUTP nick end-labeling (TUNEL) assay. Moreover, we demonstrate that CCN1/CYR61 sequesters TGF-β, resulting in decreased TGF-β signaling and fibrogenesis while Ad5-CMV-CCN1/CYR61 *in vivo* mitigated liver fibrosis in a bile duct ligation model.

2. Material and methods

2.1. Liver cells and cell lines

pMF were isolated from male Sprague–Dawley rats with a weight of 500–750 g as described previously [16]. Rats were anesthetized with ketamine and xylazine following exploratory laparotomy and the liver perfused *in situ* with collagenase (300 mg/l, Worthington, Lakewood, NJ). Hepatic hilum was removed manually from dissociated parenchymal elements and digested serially with a 0.25% pronase (Merck, Darmstadt, Germany) and 0.1% hyaluronidase (Sigma, Taufkirchen, Germany) solution and cell suspensions filtered through a 100 μm-pore mesh. The resulting suspension of non-parenchymal cells was plated for 24 h in Dulbecco's modified medium/F-12 with 3% fetal calf serum (FCS) and then supplemented to 10% FCS. Upon culturing, portal fibroblasts did differentiate into pMF and showed microscopic appearance of spindle morphology and were positive for fibulin-2 [17] and α-SMA and negative for desmin [18]. Primary HSC were isolated from male Sprague–Dawley rats through density gradient centrifugation technique and cultured as described [19,20]. MFB were obtained by sub-cultivation of HSC at day 7 of initial culturing.

2.2. RNA isolation, cDNA synthesis, and qRT-PCR

Total RNA from HSC/MFB and immortalized rat CFSC-2G cells [21] was isolated through QIAzol lysis reagent and RNeasy Mini kits (Qiagen, Hilden, Germany) according to manufacturer's instructions. RNA from liver was isolated according to a guanidine thiocyanate/CsCl method [22], followed by DNAse digestion and subsequent RNeasy clean up. Primers for amplification were selected from sequences deposited in the GenBank database (Table A1) using the Primer Express software (Applied Biosystems Invitrogen, Darmstadt, Germany). First-strand cDNA was synthesized from 1 to 2 μg RNA in 20 μl volume using SuperScript™ II reverse transcriptase and random hexamer primers (Invitrogen). To allow semi-quantitative analysis of mRNA expression, cDNAs were amplified at low cycle numbers in the range of linear amplification. For quantitative real-time PCR, cDNA derived from 25 ng RNA was amplified in 25 μl volume using qPCR Core Kits (Eurogentec, Cologne, Germany). PCR conditions were set to 50 °C for 2 min, 40 cycles at 95 °C for 15 s and 60 °C for 1 min. All TaqMan primers used in this study are given in Table A1. RNA normalization was achieved through TaqMan Ribosomal RNA Control Reagents (Applied Biosystems) designed for 18S ribosomal RNA (rRNA) detection.

2.3. Overexpression of CCN1/CYR61 in CFSC

For transient overexpression of CCN1/CYR61, we used the expression plasmid IRAKp961O1410Q (imaGenes, Berlin, Germany) containing full-length cDNA of murine CCN1/CYR61. For transfection, cells were seeded in 6-well plates one day before transfection in Dulbecco's Modified Eagle Medium (DMEM) containing 10% FCS, 4 mM L-glutamine, 100 IU/ml penicillin, and 100 μg/ml streptomycin, while non-essential amino acids were added for CFSC. Prior to transfection, the medium was renewed and cells were transfected with 2 μg vector each using the Mirus transfection reagent (Mirus, VWR International GmbH, Darmstadt, Germany) in accordance with manufacturer's instructions.

2.4. Cloning of the adenoviral expression vector AdEasy-1-CMV-mCCN1/mCYR61

The full-length cDNA of murine CCN1/CYR61 of clone IRAKp961O1410Q was released by a *Kpn*I/*Not*I cut and cloned into adenoviral shuttle vector pShuttle-CMV that was cut by the same enzymes resulting in vector pShuttle-CMV-mCCN1/mCYR61. The integrity of this vector was proven by sequencing (Fig. A1) and restriction site analysis. Thereafter, the shuttle vector was linearized by digest with *Pme*I and the CMV-mCCN1/mCYR61 expression cassette was transferred by homologous recombination in BJ5183 cells into the AdEasy-1 backbone vector using standard protocols. Two individual recombinants of AdEasy1-CMV-mCCN1/mCYR61 (*i.e.* Ad5-CMV-CCN1-2 and Ad5-CMV-CCN1-8)

were further propagated in HEK cells and purified by a two-step purification protocol using CsCl centrifugation and the Adeno-X Maxi Purification kit (Clontech, Mountain View, CA).

2.5. Adenoviral gene transfer into primary pMF

Primary pMF were used up to the 4th passage. For infection, they were incubated for 24 h with 2×10^9 virions/ml of Ad5-CMV-CCN1 or the viral control Ad5-CMV-Luc expressing luciferase. Following adenoviral transduction, the medium was changed and cells were maintained in DMEM/F12 under normal growth condition (10% FCS) for indicated periods following assessment of CCN1/CYR61 induced cellular senescence, apoptosis and antifibrotic effects.

2.6. SDS-PAGE and Western blot analysis

Cell and tissue lysates were prepared using RIPA buffer containing 20 mM Tris–HCl (pH 7.2), 150 mM NaCl, 2% (w/v) NP-40, 0.1% (w/v) SDS, 0.5% (w/v) sodium deoxycholate and the Complete™-mixture of proteinase inhibitors (Roche, Mannheim, Germany). Equal amounts of cellular protein extracts or supernatants were diluted with Nu-PAGE™ LDS electrophoresis sample buffer with DTT as reducing agent, heated at 95 °C for 10 min, and separated in 4–12% Bis–Tris gradient gels and 10% Bis–Tris gels, using MOPS or MES running buffer (Invitrogen). Proteins were electroblotted on nitrocellulose membranes, and equal loading was shown in Ponceau S stain. Subsequently, non-specific binding sites were blocked in TBS containing 5% (w/v) non-fat milk powder. All antibodies (Table A2) were diluted in 2.5% (w/v) non-fat milk powder in Tris-buffered saline. Primary antibodies were visualized using horseradish peroxidase conjugated anti-mouse, anti-rabbit or anti-goat IgG (Santa Cruz Biotech, Santa Cruz, CA) and the SuperSignal chemiluminescent substrate (Pierce, Bonn, Germany).

2.7. Animal experiments and specimen collection

All animal protocols were in compliance with the guidelines for animal care approved by the German Animal Care Committee. Sprague–Dawley rats were subjected to BDL as described previously [23], and sacrificed at indicated time points. Liver specimen was snap frozen in liquid nitrogen for protein and RNA isolation or fixed in 4% buffered

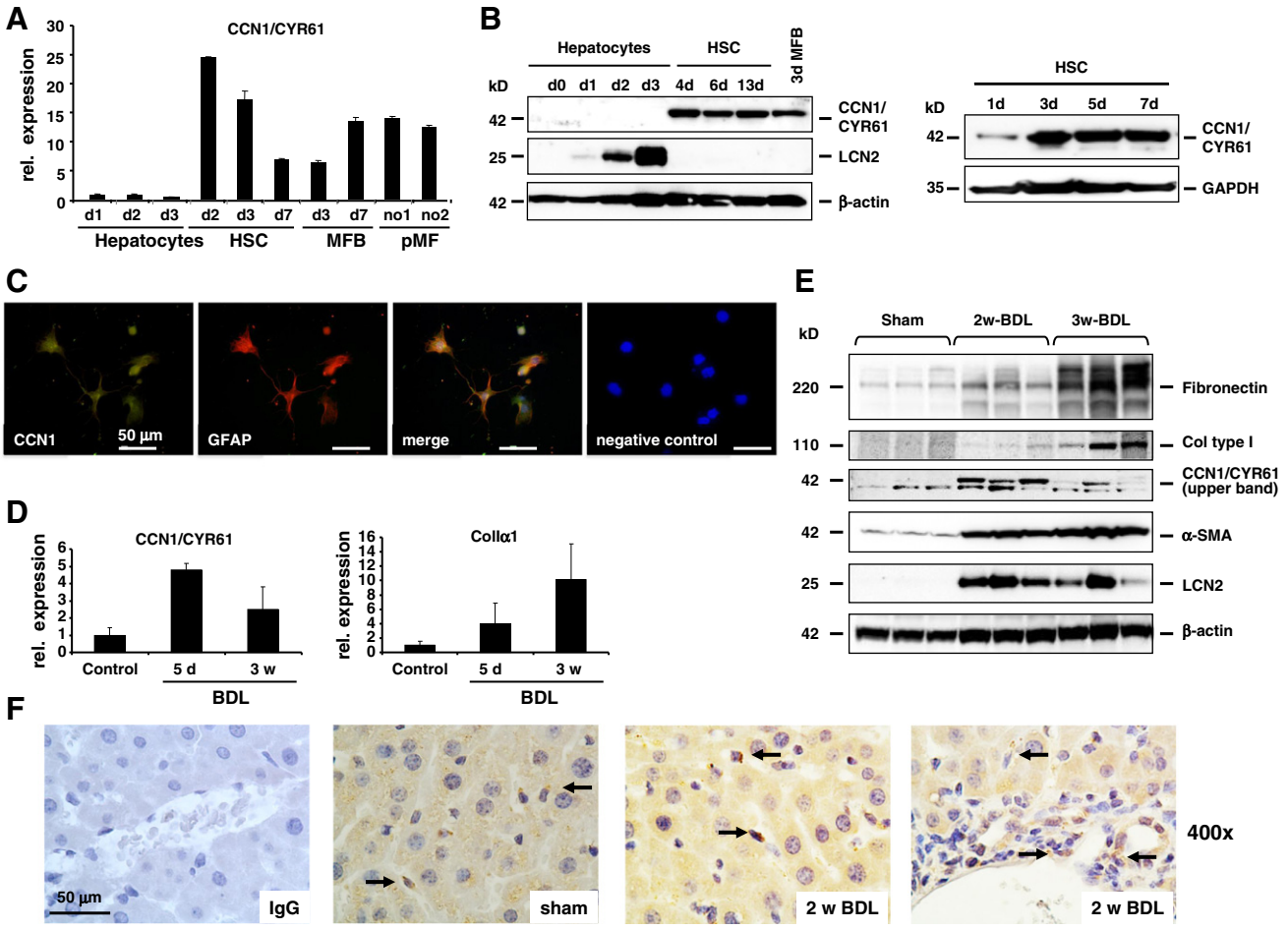

Fig. 1. Expression analysis of CCN1/CYR61 in primary cultured hepatic cell subpopulations and experimental liver injury models. (A) Quantitative real-time PCR analysis of CCN1/CYR61 in hepatocytes (cultured for 1, 2, and 3 days), hepatic stellate cells (cultured for 2, 3, and 7 days), fully transdifferentiated MFB (cultured for 3 or 7 days) and two different isolates of passage portal myofibroblasts (pMF). (B) Western blot analysis of protein lysates from hepatocytes, HSC and MFB cultured for indicated periods, using antibodies directed against CCN1/CYR61 and LCN2, while expression of β-actin and GAPDH served as loading controls. (C) Immunocytochemistry of HSC cultured for one day showing expression of CCN1/CYR61 and GFAP, a specific marker of HSC. (D) Quantitative real-time PCR of CCN1/CYR61 hepatic expression (*left panel*) and collagen type I (*right panel*) in livers of animals, 5 days or 3 weeks after BDL. (E) Western blots of liver protein extracts prepared from control mice or animals subjected to BDL for 2 or 3 weeks and probed with antibodies specific for fibronectin, collagen type I, CCN1/CYR61 (sc-13100), α-SMA, LCN2 and with β-actin as loading control. (E) Immunohistochemistry of liver sections taken from controls and 2-week BDL animals, both showing CCN1/CYR61 positive staining in nonparenchymal cells (*black arrows*). IgG served as a negative control.

paraformaldehyde for histology. For the CCl_4 treatment, male Sprague–Dawley rats weighing 180–200 g received intraperitoneal injections of 1 ml/kg of CCl_4 in an equal volume of mineral oil twice weekly for up to 12 weeks following established protocols [24].

2.8. Immunohistochemistry

Liver tissue sections were treated as described before [24]. For CCN1/CYR61 detection, we applied a sheep anti-mouse CCN1/CCYR61 antibody (AF4055; R&D Systems, Wiesbaden, Germany) overnight. Liver slides were incubated with biotinylated secondary antibodies (DAKO, Hamburg, Germany) and developed with the Vectastain ABC-Elite reagent (Vector Laboratories, Eching, Germany) and peroxidase substrate 3,3′-diaminobenzidine substrate (Sigma).

2.9. Fluorescent immunocytochemistry

pMF cultured on coverslips were fixed at indicated time points with 4% paraformaldehyde in PBS for 15 min at room temperature, followed by a 5 min permeabilization step with 0.3% TritonX-100 and 0.1% sodium citrate (pH 6) on ice. Coverslips were then blocked with 50% FCS, 1% BSA and 0.025% Tween 20 in PBS for 30 min at 37 °C, followed by 4 °C overnight incubation with primary antibodies. Subsequently, the Alexa Fluor® conjugate secondary antibodies were applied for 1 h at room temperature and the nuclei were counterstained with 4′,6-diamidino-2-phenylindole (DAPI). Finally, the coverslips were mounted on glass slides and analyzed by fluorescence microscopy. This protocol was also applied for fluorescence double staining of liver cryosections.

2.10. Detection of cellular senescence

To measure cellular senescence, the activity of β-galactosidase (β-Gal) was measured at pH 6 using the Senescence β-Galactosidase Staining Kit (#9860) obtained from Cell Signaling Technology (NEB, Frankfurt, Germany), essentially following manufacturer's instructions.

2.11. Terminal transferase dUTP nick end-labeling assay (TUNEL)

For DNA fragmentation detection resulting from apoptotic signaling cascades, we used the *In Situ* Cell Death Detection Kit Fluorescein (Roche) according to manufacturer's instructions. The presence of nicks in the DNA was identified by terminal deoxynucleotidyl transferase (TdT), an enzyme that catalyzes the addition of labeled dUTPs. Cultured pMF on glass coverslips were analyzed by fluorescence microscopy for direct fluorescein. For positive control staining, the specimens were digested with DNAse.

2.12. Reactive oxygen species (ROS) detection

The formation of ROS was analyzed with the Reactive Oxygen Species Detection Reagents (Invitrogen). In this assay system, the carboxyl derivative of fluorescein (10 μM CM-H_2DCFDA, Invitrogen) was applied as cell-permeated indicator dye for ROS in cultured pMF on glass slides for 30 min. The chemically reduced and acetylated forms of 2′,7′-dichlorofluorescein (DCF) and calcein are non-fluorescent until the acetate groups are removed by intracellular esterases and oxidation occurs within the cell. Esterase cleavage of the lipophilic blocking groups yields a charged form of the dye that can be visualized by fluorescence microscopy. For ROS *in situ* quantitative analysis, cells were cultured in 96 well plates and the fluorescence measured by microplate reader

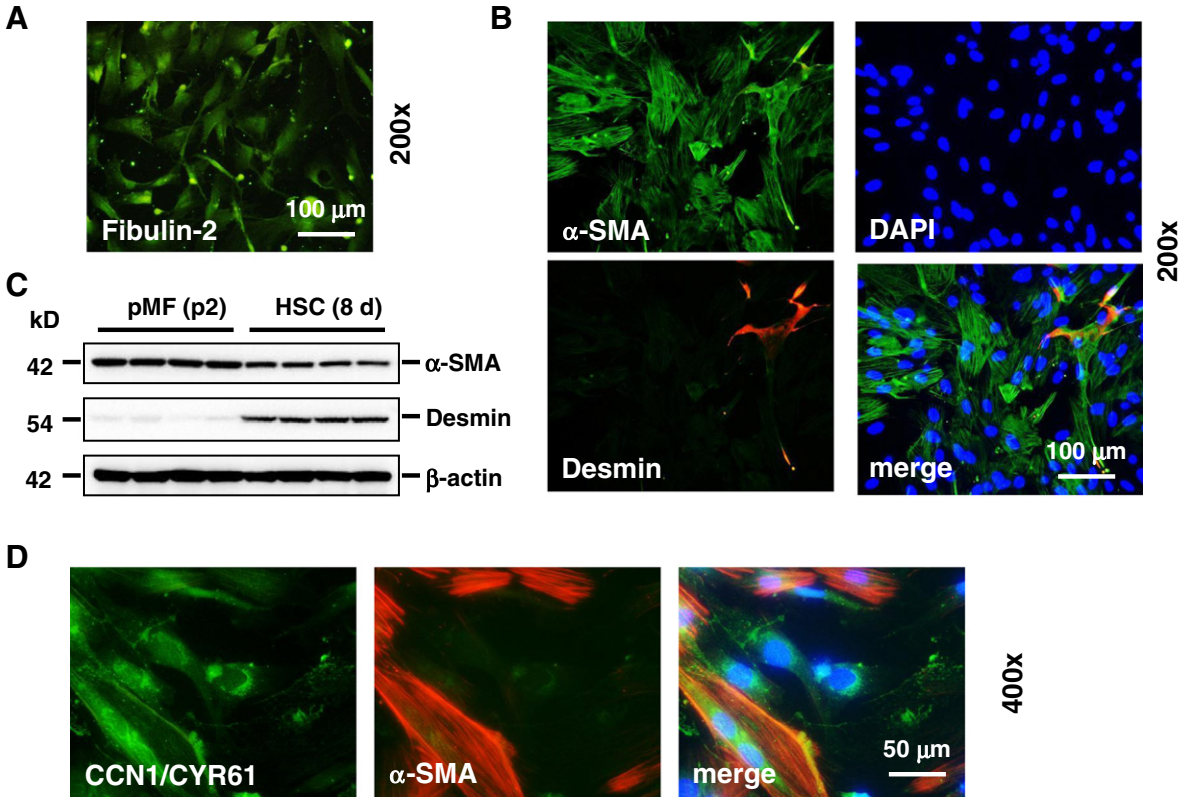

Fig. 2. Characteristics of primary pMF in culture. (A) Immunohistochemistry of primary pMF cultured on glass coverslips showed positive staining of fibulin-2. (B) pMF at passage 2 (*p2*) express α-SMA, but are negative for desmin. (C) Foregoing was duly confirmed in Western blot analysis. (D) CCN1/CYR61 expression was found to localize in the endoplasmic reticulum around the nucleus in cultured differentiated pMF. Cells expressing high levels of CCN1/CYR61 notably showed reduced α-SMA expression.

(Victor 1420 multilabel counter from Wallac, Turku, Finland) and the values normalized with cellular DNA.

2.13. Luciferase reporter gene assay

Experiments were performed in 6-well plates. Confluent pMF cells in 4% FCS were transduced with Ad5-$(CAGA)_{12}$-MLP-Luc followed by Ad5-CMV-CCN1 12 h later. Cells were starved for 16 h in medium containing 0.5% FCS and renewed with 0.2% FCS and 1 mg/ml BSA before stimulation with TGF-β at indicated doses for 12 h. Cell extracts were prepared in 350 μl of passive lysis buffer (Promega), and 20 μl was used for luciferase measurements. All experiments were conducted in triplicate.

2.14. CCN1/CYR61-Fc chimera/TGF-β1 co-immunoprecipitation

Samples for co-immunoprecipitation (co-IP) containing recombinant human CCN1/CYR61-Fc chimera (#4055-CR-050) and recombinant human TGF-β1 (240-B-002) were obtained from R&D Systems, and set up in a total volume of 400 μl PBS, rotated for 6 h at 4 °C, then 20 μl Protein-G PLUS agarose beads equilibrated in PBS (Santa Cruz Biotech, Santa Cruz, CA) were added and the mixture rotated overnight at 4 °C. Aliquots (30 μl) were taken without further treatment (−Protein G precipitation) and the remaining 370 μl was subjected to standard Protein G precipitation (+Protein G precipitation). Protein G beads were collected by brief centrifugation and washed three times in ice cold PBS. Samples were run on a Pre-Cast NUPAGE 4–12% polyacrylamide gel under reducing conditions with MES running buffer (Invitrogen, Life Technologies, Darmstadt, Germany). Detection of TGF-β1 was achieved with antibody CS#3711 (Cell Signaling, New England Biolabs, Frankfurt, Germany) and CCN1/CYR61-Fc chimera was detected using an affinity purified polyclonal sheep antibody (AF4055) directed against murine CCN1/CYR61 (R&D Systems). Recombinant CCN1/CYR61-Fc chimera and TGF-β1, not subjected to any further treatment, served as Western blot controls. A recombinant fusion protein harboring the platelet-derived growth factor receptor type β and the Fc part served as a further control in this set of experiments. The construction and purification of this protein chimera was reported in detail elsewhere [25].

2.15. Statistics

Data are expressed as mean ± standard deviation (SD). Means of different groups were compared using 1-way analysis of variance. Statistical analysis was performed using the unpaired Student's *t* test. Probability values of less than 0.05, 0.01 and 0.001 were considered as statistically significant and marked with "*", "**" and "***".

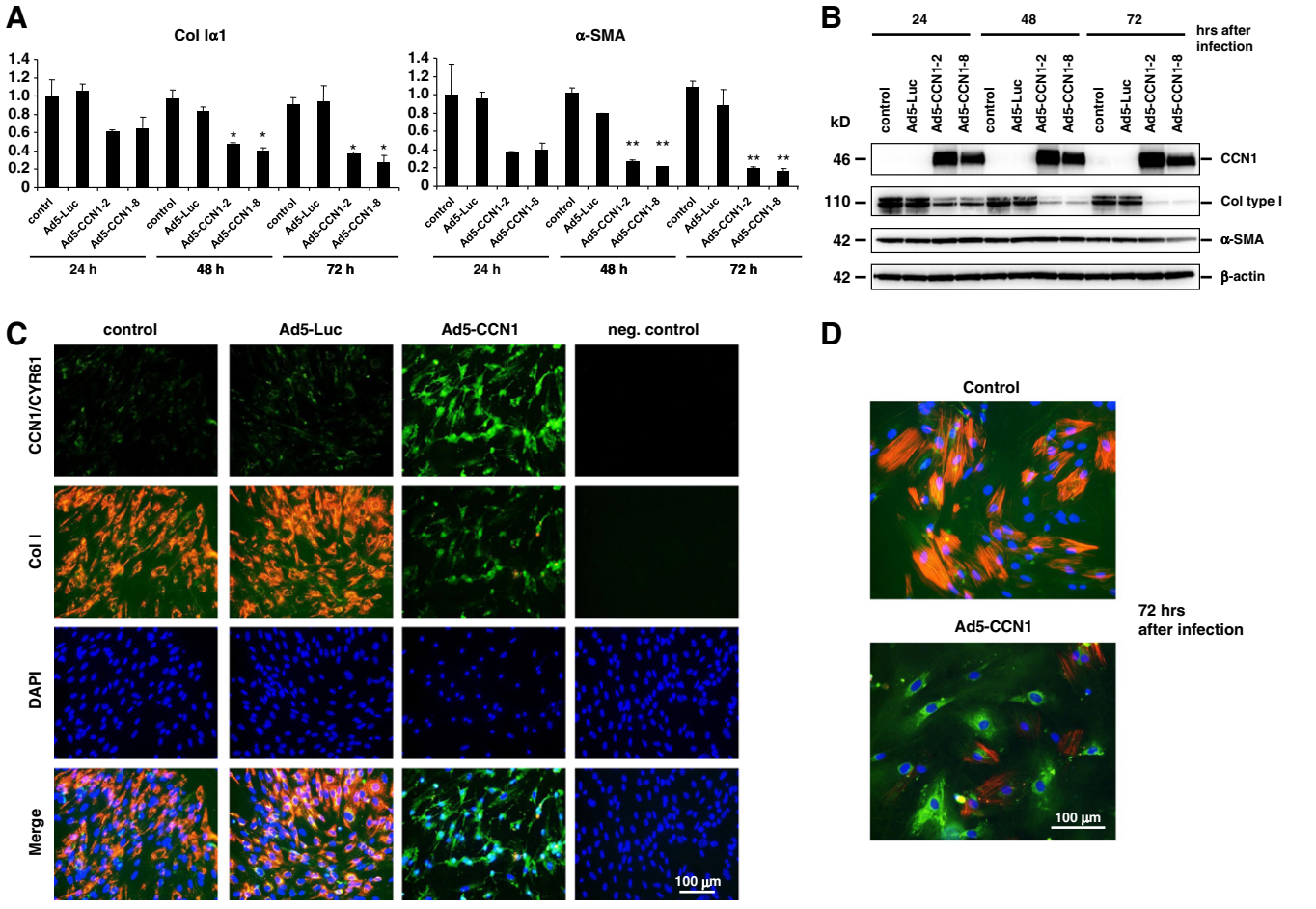

Fig. 3. Ad5-CMV-CCN1 infection induces reduced expression of collagen type I and α-SMA in pMF. (A) Quantitative real-time PCR showing markedly decreased expression of collagen type I and α-SMA mRNA upon transduction with Ad5-CMV-CCN1. (B) Western blot analysis confirmed the suppressive effects of CCN1/CYR61 on col type I protein, while α-SMA expression was only marginally affected. ß-actin served as loading control. (C) Immunocytochemistry double staining of CCN1/CYR61 (*green*) and collagen type I (*red*) of cultured pMF following 72 h Ad5-CMV-CCN1 transduction showing Ad5-CMV-CCN1 to significantly inhibit collagen type I expression in pMF. Staining with non-immune IgG control serum served as a negative control. (D) Immunocytochemistry double staining of CCN1/CYR61 (*green*) and α-SMA (*red*) of early period cultured pMF after 72 h Ad5-CMV-CCN1 infection, showing Ad5-CMV-CCN1 to efficiently inhibit α-SMA expression.

3. Results

3.1. CCN1/CYR61 expression in isolated primary liver cells

In fibrotic livers, HSC and pMF are considered the main producers of ECM [8,9]. In culture, primary HSC get activated and transdifferentiate in a time-dependent manner from a quiescent phenotype into a proliferative active contractile phenotype (*i.e.*, MFB). We used qRT-PCR and Western blot to analyze CCN1/CYR61 expression during cellular activation and transdifferentiation, both revealing a dramatic CCN1/CYR61 increase during initial HSC activation, followed by a subsequent decline in fully transdifferentiated MFB and comparable to the CCN1/CYR61 levels in passaged pMF. By contrast, CCN1/CYR61 expression in primary hepatocytes in both qRT-PCR and Western blot was relatively minor compared to HSC, MFB and pMF, while lipocalin 2 (LCN2), known to be induced during prolonged culturing of hepatocyte, showed a marked upregulation (Fig. 1A, B). Immunofluorescent double staining of GFAP, a marker of HSC, and CCN1/CYR61 was confirmed in primary HSC that were cultured for one day after isolation (Fig. 1C).

3.2. Expression of CCN1/CYR61 in experimental fibrotic models

Next, we investigated CCN1/CYR61 expression in two different *in vivo* models of hepatic fibrogenesis using qRT-PCR of liver RNA samples and Western blot analysis of protein extracts isolated from rats subjected to BDL surgery and CCl_4 treatment. In agreement with

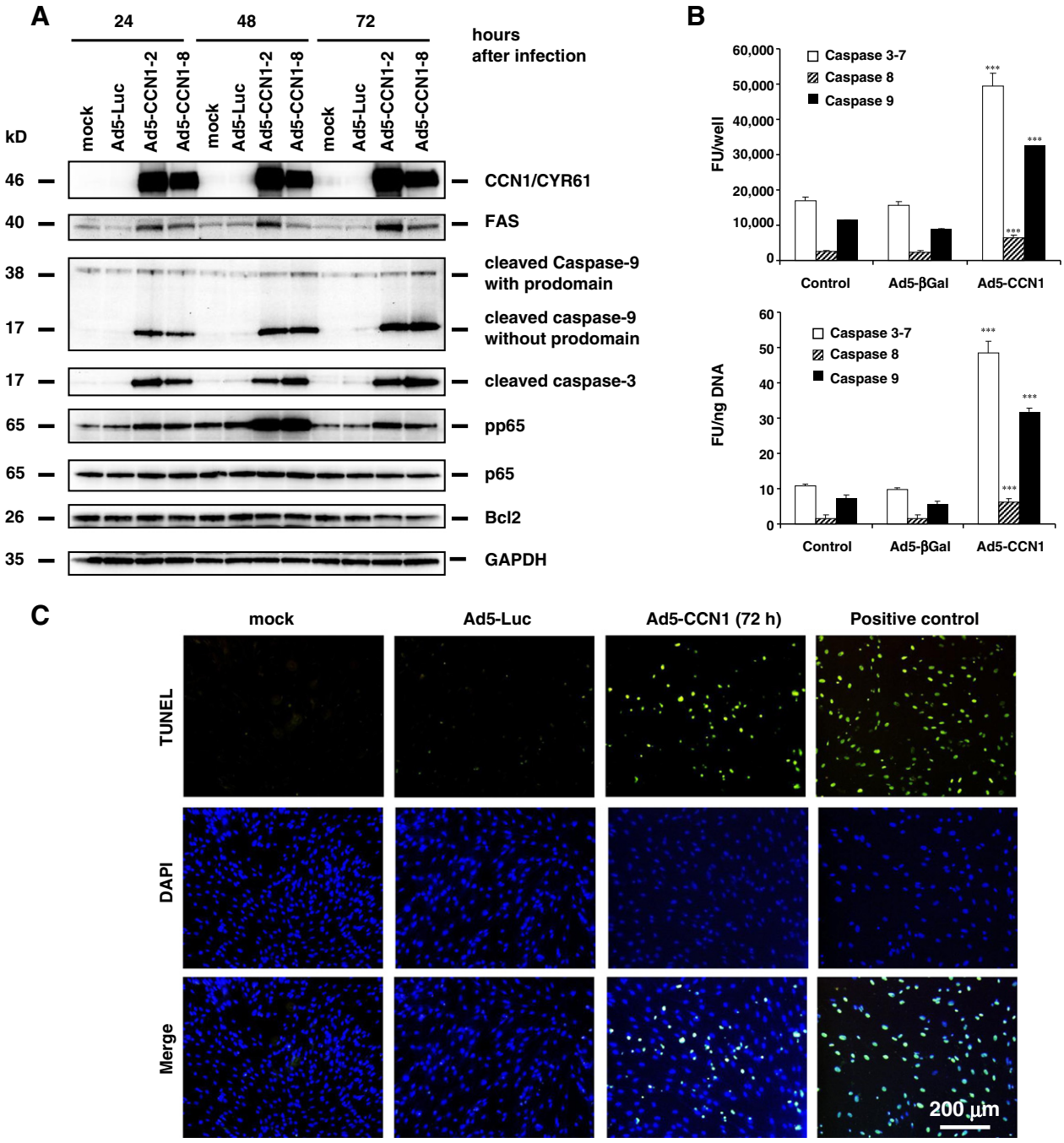

Fig. 4. Ad5-CMV-CCN1 induces pMF apoptosis. (A) Western blot analysis revealed that overexpression of CCN1/CYR61 leads to increased expression of apoptotic marker proteins, including cleaved caspase-9 and -3 and FAS. Pro-survival factor NFκB (p65) also showed significant activation, while Bcl2 decreased slightly. GAPDH served as loading control. (B) Quantitative caspase activity showing significant upregulation of all caspases. (C) TUNEL assay confirming fluorescent nuclear staining of apoptotic cells in Ad5-CMV-CCN1/CYR61 transduced pMF.

the *in vitro* expression kinetics, this analysis revealed the expression of CCN1/CYR61 to increase, especially during the early phases of injury while declining thereafter. Compared to sham-operated rats, we particularly noticed an increase of CCN1/CYR61 two weeks after setting of the BDL surgery and subsequently decreased at later stages. Initial CCN1/CYR61 upregulation showed correspondence with the expression of α-smooth muscle actin (α-SMA), collagen type I (col1α1) and the acute phase response protein LCN2 (Fig. 1D, E). CCl_4 injection

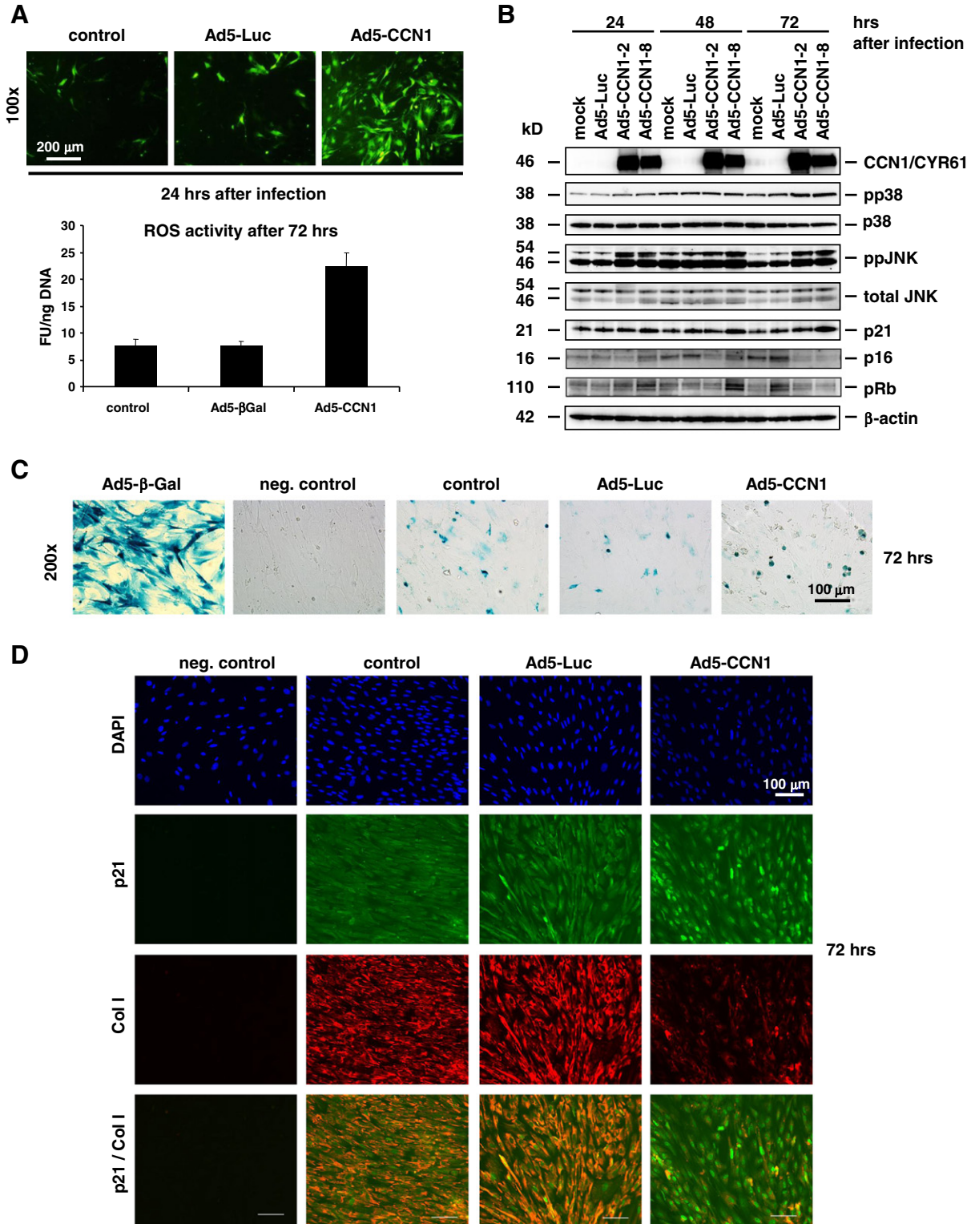

Fig. 5. Reactive oxygen species (ROS) detection. (A) ROS formation in viable cultured pMF was analyzed with ROS detection reagent (*upper panel*), showing Ad5-CMV-CCN1/CYR61 infection to induce significantly ROS production in pMF. The quantitative ROS assay (*lower panel*) was performed after 72 h infection. (B) Western blot analysis revealed Ad5-CMV-CCN1 to induce p38 and JNK phosphorylation with slightly increased expression of p21. ß-actin served as loading control in this analysis. (C) β-Galactosidase staining for cellular senescence was positive in both control cultures and Ad5-CMV-CCN1 infected cells, but Ad5-CMV-CCN1 did induce pMF detachment and apoptosis. Cultured pMF infected with Ad5-CMV-βGal served as positive control. (D) Immunocytochemistry double staining of p21 (*green*) and collagen type I (*red*) revealed nuclear localization of p21 and reduced col I expression in pMF infected with Ad5-CMV-CCN1.

reflected the same phenomenon, with dramatic upregulation of CCN1/CYR61 upon initial application, decreasing following long-term application and liver fibrosis (Fig. A2A and B). CCN1/CYR61 immunohistochemistry of specimens taken from rat livers subjected to BDL and CCl_4 showed positive staining in non-parenchymal cells, *i.e.* HSC and pMF (Fig. 1F and Fig. A2C). Immunofluorescent double staining showed high background in parenchymal cells, with a stronger positive signal in perisinusoidal areas and minimal co-localization with collagen type I positive cells (Fig. A2D).

3.3. Characteristics of isolated primary pMF

Immunocytochemistry of cultured primary pMF showed positive staining of fibulin-2, a specific marker of this hepatic cell subpopulation (Fig. 2A). Compared to its HSC counterpart, pMF do express α-SMA but are negative for desmin, as confirmed by both immunohistochemistry and Western blot analysis (Fig. 2B and C). In early periods of culturing, CCN1/CYR61 was found to localize mainly in the endoplasmic reticulum around the nucleus, while more differentiated pMF expressed overall lower levels of CCN1/CYR61, combined with higher levels of α-SMA filament (Fig. 2D).

3.4. Ad5-CMV-CCN1 decreased collagen type I and α-SMA expression in pMF

Cultured pMF at passage 2 were infected with Ad5-CMV-CCN1 for 24, 48 and 72 h and analyzed for expression of col1α1 and α-SMA by qRT-PCR. Interestingly, the overexpression of CCN1/CYR61 resulted in markedly decreased expression of both col1α1 and α-SMA mRNA (Fig. 3A). Ad5-CMV-CCN1 mediated gene transfer in pMF triggered very high level expression of CCN1/CYR61 (Fig. 3B) in both cell lysate and culture supernatant (data not shown). Western blot confirmed the qRT-PCR analysis, showing overexpression of CCN1/CYR61 to significantly reduce collagen type I production, with only a marginal impact of CCN1/CYR61 on α-SMA protein expression (Fig. 3B). Immunohistochemistry also confirmed the overexpression of CCN1/CYR61 in the respective cells and to inhibit col1α1 production (Fig. 3C). Foregoing was confirmed in Ad5-CMV-CCN1 transduced primary HSC (Fig. A3A) and plasmid transfected CFSC (Fig. A3B). Interestingly, overexpression of CCN1/CYR61 through Ad5-CMV-CCN1 in early stage of pMF was able to inhibit α-SMA expression (Fig. 3D).

3.5. Ad5-CMV-CCN1 induced pMF apoptosis

We further found overexpression of CCN1/CYR61 in pMF to correlate with an increase of apoptotic marker proteins such as FAS and cleaved caspase-3 and -9 (Fig. 4A). Ad5-CMV-CCN1 transduced pMF also showed a significant increase in TUNEL positive cells compared to control culture or Ad5-CMV-Luc-infected cells (Fig. 4B). Moreover, quantitative values for caspase activity increased significantly for all types of caspases (Fig. 4C), but more prominent for caspase 9 and 3–7 compared to caspase 8.

3.6. Ad5-CMV-CCN1 induced ROS production and activation of p38 and JNK in pMF

To test if transient overexpression of CCN1/CYR61 results in elevated intracellular ROS levels, we performed ROS staining in pMF 24 h after infection. The transduction of CCN1/CYR61 resulted in a marked increase of ROS production relative to normal cultures or Ad5-CMV-Luc infected cells, as confirmed by quantitative analysis (Fig. 5A). Additionally, adenoviral infection with Ad5-CMV-CCN1 induced p38 and JNK phosphorylation (Fig. 5B).

3.7. Ad5-CMV-CCN1 showed no difference in β-galactosidase (β-Gal) staining

Passaged cultured pMF in 10% FCS showed senescence in normal cultures including Ad5-CMV-Luc-infected and Ad5-CMV-CCN1-infected cells (Fig. 5C). Compared to all other culture conditions however, Ad5-CMV-CCN1 infected pMF showed the highest degree of cell detachment (Fig. 5C). The levels of p21 representing a marker of cellular senescence increased slightly in Ad5-CMV-CCN1 transduced pMF cells (Fig. 5B). Interestingly, Ad5-CMV-CCN1 transduced pMF showed marked nuclear localization of p21 with decreased collagen type I expression (Fig. 5D).

3.8. CCN1 protein and Ad5-CMV-CCN1 conditioned medium attenuated collagen type I expression through cellular senescence

pMF incubated with different doses of CCN1-Fc protein in 0.5% FCS for 96 h or in conditioned media taken from Ad5-CMV-CCN1 infected pMF were analyzed for CCN1/CYR61 protein and collagen type I (Fig. 6). Recombinant CCN1-Fc and conditioned medium reduced collagen type I expression in a dose-dependent manner (Fig. 6A, B, D). CCN1 protein induced phosphorylation of p65 and LCN2 expression with decreased levels of cleaved caspase 3. Several cellular senescence markers, including pp53, p21 and p16 were upregulated while showing a decreased hyperphosphorylated form of Rb (Fig. 6B). β-Gal stain was positive in normal cultures, but more prominent in pMF incubated with CCN1-Fc protein (Fig. 6C). Ad5-CMV-CCN1 infected pMF conditioned media showed the same effects as the CCN1-Fc chimera, but the conditioned media contained higher levels of CCN1 protein (data not shown) resulting in slightly increased caspase 3 cleavage, as confirmed by Western blot and quantitative caspase assay (Fig. 6D and E).

3.9. CCN1 attenuates TGF-β signaling through physically interacting with TGF-β

Ad5-CMV-CCN1-infected cells showed a dramatical decrease in collagen type I expression. Since TGF-β is the most prominent growth factor in collagen I production, we next investigated the effects of CCN1 on TGF-β signaling in pMF and found both Ad5-CMV-CCN1 expressed and recombinant CCN1 protein to attenuate Smad protein phosphorylation, including pSmad1/5/8, pSmad2 and pSmad3 (Fig. 7A and B). The luciferase reporter gene assay (CAGA-luciferase) duly confirmed the Western blot results (Fig. 7C). A binding assay of CCN1-Fc protein and TGF-β following immunoprecipitation of the CCN1-Fc chimera proved the CCN1 protein to bind to TGF-β (Fig. 7D), while an irrelevant protein consisting of the extracellular domain of the platelet-derived growth factor receptor type β and the Fc part was unable to bind to TGF-β under the chosen experimental conditions.

3.10. Ad5-CMV-CCN1 attenuated liver fibrosis in the BDL model

Since pMF play an essential role in biliary fibrotic models [26,27], 2-week-sham and BDL animals were treated with Ad5-CMV-CCN1 (1×10^{10} virions/animal/week). In this analysis, Ad5-CMV-GFP was used as the viral vector control. In liver, both adenoviral constructs effectively transduced parenchymal and non-parenchymal liver cells (Fig. 8A). The Ad5-CMV-CCN1 treated group showed significant decreased collagen type I and α-SMA levels in Western blot, Sirius red and immunohistochemistry (Fig. 8B, C, and D). ROS staining in respective liver sections further showed the occurrence of elevated concentrations of ROS in animals that received Ad5-CMV-CCN1 (Fig. 8E and F). Moreover, senescence β-galactosidase staining reflected positive signals around portal areas in all BDL livers, with Ad5-CMV-CCN1 showing the strongest signals (Fig. 8E and F). Foregoing findings concur with a recent publication showing that the CCN1/CYR61 promotes regression of liver fibrosis through induction of cellular senescence in hepatic myofibroblasts [28]. Additionally,

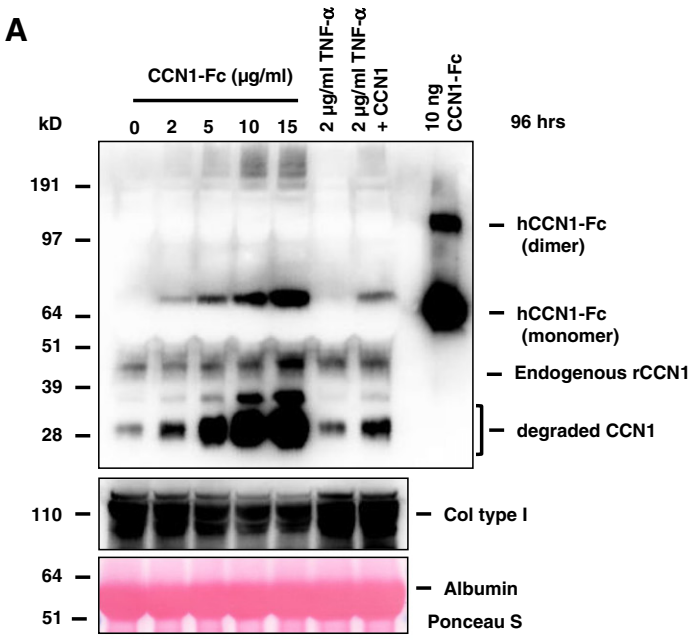
A
CCN1-Fc (μg/ml)
kD
0 2 5 10 15
2 μg/ml TNF-α
2 μg/ml TNF-α + CCN1
10 ng CCN1-Fc
96 hrs
191
97
64
51
39
28
110
64
51
hCCN1-Fc (dimer)
hCCN1-Fc (monomer)
Endogenous rCCN1
degraded CCN1
Col type I
Albumin
Ponceau S

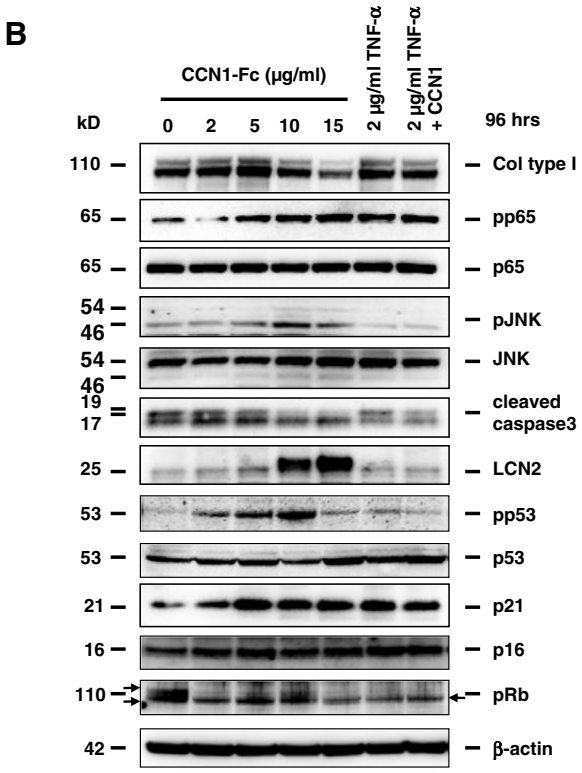
B
CCN1-Fc (μg/ml)
kD
0 2 5 10 15
2 μg/ml TNF-α
2 μg/ml TNF-α + CCN1
96 hrs
110
65
65
54
46
54
46
19
17
25
53
53
21
16
110
42
Col type I
pp65
p65
pJNK
JNK
cleaved caspase3
LCN2
pp53
p53
p21
p16
pRb
β-actin

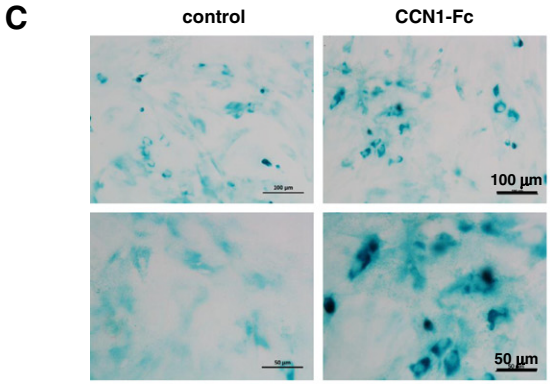
C
control
CCN1-Fc
100 μm
50 μm

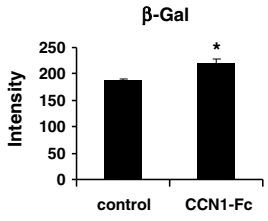
β-Gal
Intensity
250
200
150
100
50
0
*
control
CCN1-Fc

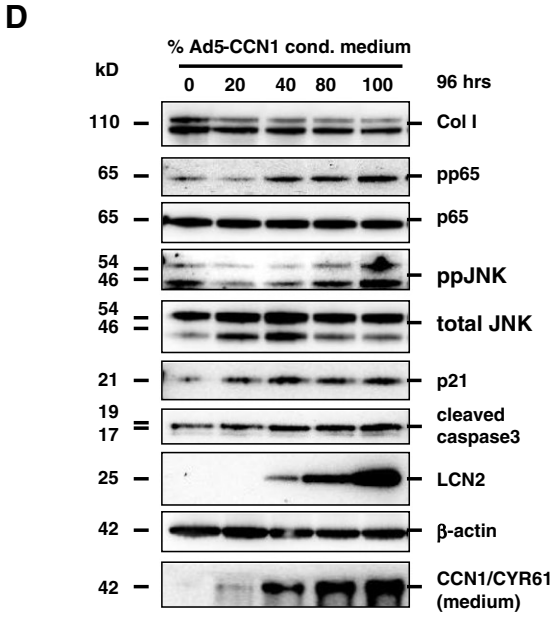
D
% Ad5-CCN1 cond. medium
kD
0 20 40 80 100
96 hrs
110
65
65
54
46
54
46
21
19
17
25
42
42
Col I
pp65
p65
ppJNK
total JNK
p21
cleaved caspase3
LCN2
β-actin
CCN1/CYR61 (medium)

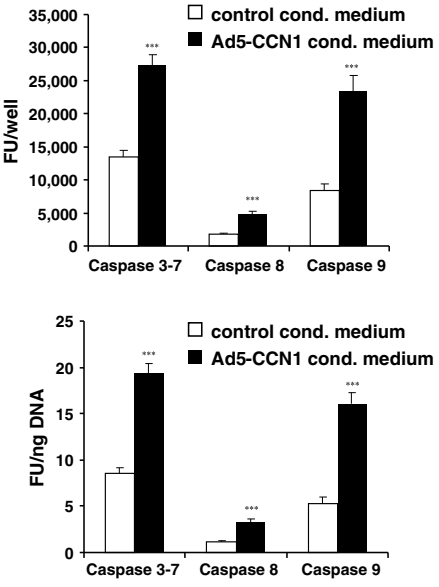
E
control cond. medium
Ad5-CCN1 cond. medium
FU/well
35,000
30,000
25,000
20,000
15,000
10,000
5,000
0
Caspase 3-7
Caspase 8
Caspase 9
FU/ng DNA
25
20
15
10
5
0

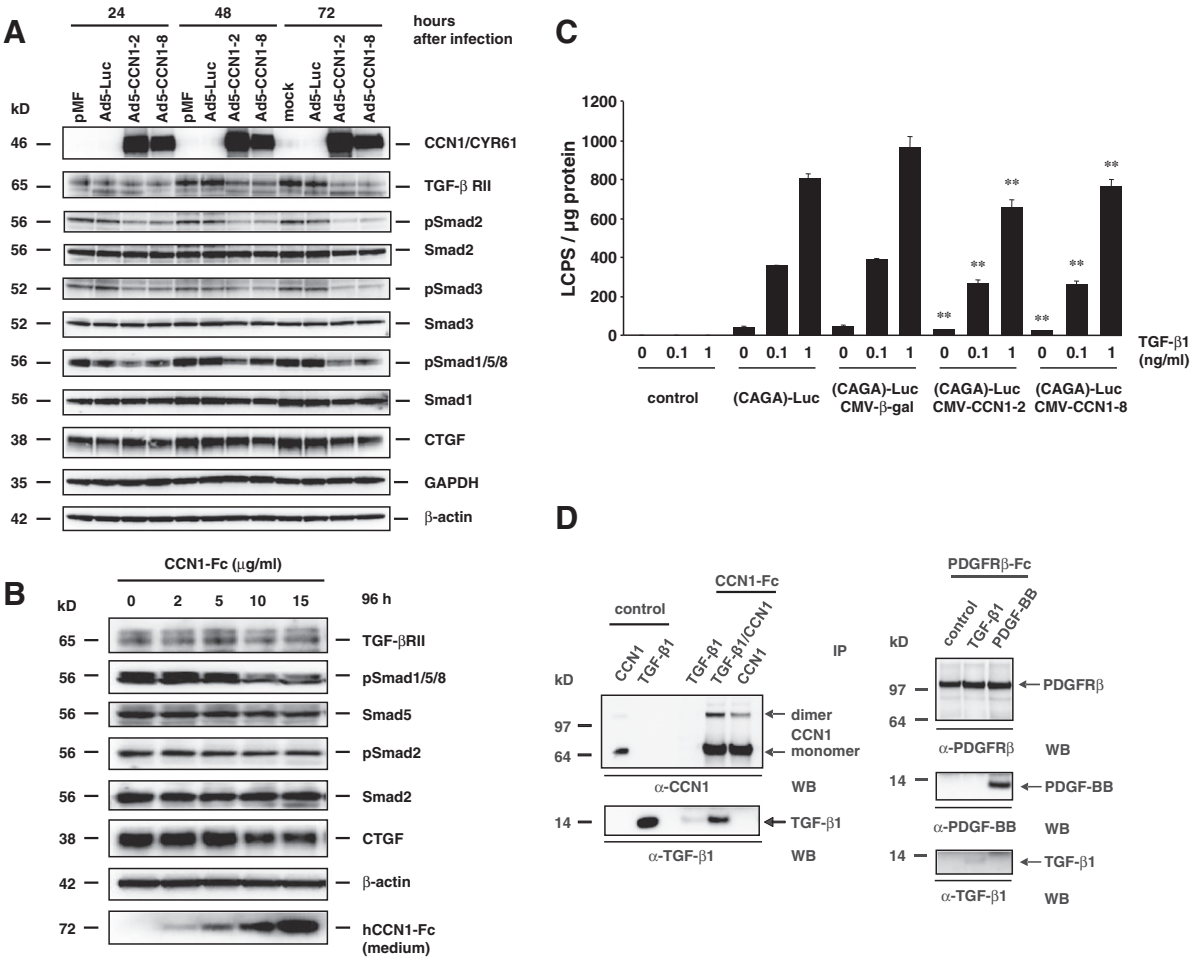

Fig. 7. CCN1 and TGF-β signaling. (A) Western blot analysis of pMF treated as indicated, reflecting Ad5-CMV-CCN1 transduced cells to decrease TGF-β receptor type II, pSmad1/5/8, pSmad2 and pSmad3 and the TGF-β gene target CTGF. High CCN1 protein expression was found in Ad5-CMV-CCN1 transduced pMF. ß-actin served as loading control in this analysis. (B) Western blot analysis of pMF cell lysates from CCN1-Fc protein incubation, showing decreased TGF-β receptor type II, pSmad proteins and CTGF with β-actin as loading control. CCN1-Fc protein from the incubated media was confirmed in Western blot. (C) The luciferase reporter gene assay (CAGA-luciferase) confirmed significantly decreased CAGA-luciferase activity in pMF incubated with CCN1-Fc protein, with and without TGF-β stimulation. (D) CCN1-Fc and TGF-β binding assay following Protein-G PLUS agarose bead precipitation showing TGF-β to bind to CCN1 (*left panel*). Recombinant CCN1-Fc and TGF-β (*lanes 1 and 2*) served as positive controls for Western blots. As a further control a soluble PDGFRβ-Fc construct that has high affinity for PDGF-BB but lacks affinity for TGF-β1 was taken in this set of experiments (*right panel*).

BDL livers treated with Ad5-CMV-CCN1 showed only TUNEL positive cells around portal areas while controls and Ad5-CMV-GFP infected livers were mainly positive at the necro-apoptotic region of parenchymal cells. Furthermore, immunohistochemistry of cleaved caspase 3 was positive in hepatocytes in Ad5-CMV-GFP infected liver sections. By contrast, Ad5-CMV-CCN1 infected livers showed increased caspase 3 cleavage more prominently in non-parenchymal cells (Fig. 8E).

4. Discussion

CCN1/CYR61 is a matricellular protein of the CCN family that associates specifically with the extracellular matrix. CCN proteins lack specific high-affinity receptors, but do regulate crucial biological processes like fibrogenesis, by signaling *via* diverse integrins and proteoglycans. CCN1/CYR61 enhances cutaneous wound healing through recruitment of MFB to form the granulation tissue where they proliferate and rapidly synthesize ECM components to enforce tissue integrity during repair.

Similar to cutaneous wound healing, liver fibrosis is a tissue healing process that recruits MFB from HSC and pMF, depending on the pathogenesis of the injured liver. We found CCN1/CYR61 upregulation upon early HSC activation followed by decreasing levels in fully differentiated MFB, in line with the experimental liver fibrotic models BDL and CCl_4 showing CCN1/CYR61 levels to be in reverse to the actual degree of liver fibrosis (Fig. 1 and Fig. A2). This indicates that CCN1/CYR61 participates in tissue repair during the process of inflammation and early fibrotic tissue formation. By contrast to liver fibrosis, MFB are driven into senescence by CCN1/CYR61 in later stages of cutaneous wound healing, whereupon they transform into an ECM-degrading phenotype and thus limit fibrosis. CCN1/CYR61 therefore functions as an anti-

Fig. 6. CCN1/CYR61 protein and Ad5-CMV-CCN1 conditioned media induced pMF senescence. (A) Western blot analysis of media (40 μl/lane) taken from pMF that were incubated with indicated doses of CCN1-Fc protein for 96 h. The recombinant CCN1-Fc protein, endogenous rat CCN1/CYR61, and collagen type I expression were detected by Western blot analysis. In this analysis 10 ng of CCN1-Fc was used as positive control, while the Ponceau S stain served as control for equal protein loading. (B) Western blots of cell lysate showing CCN1-Fc to decrease collagen type I and cleaved caspase 3, but increased pp65, pJNK, pp53, p21 and LCN2. ß-actin served as loading control. Please note that the incubation with CCN1-Fc leads to hyperphosphorylation of RB protein (lower arrow) that is also induced by incubation with TNF-α. (C) β-Gal staining of pMF incubated with CCN1-Fc protein. (D) Western blots of cell lysate from pMF cultured in Ad5-CMV-CCN1 conditioned media, showing decreased levels of collagen type I, with increased pp65, pJNK, p21, LCN2 and cleaved caspase 3. Significant levels of CCN1 were found in the conditioned media. ß-actin served as loading control. (E) Quantitative caspase activity showing significant increases in all types of caspases. Control conditioned media were taken from the parallel normal cultured pMF.

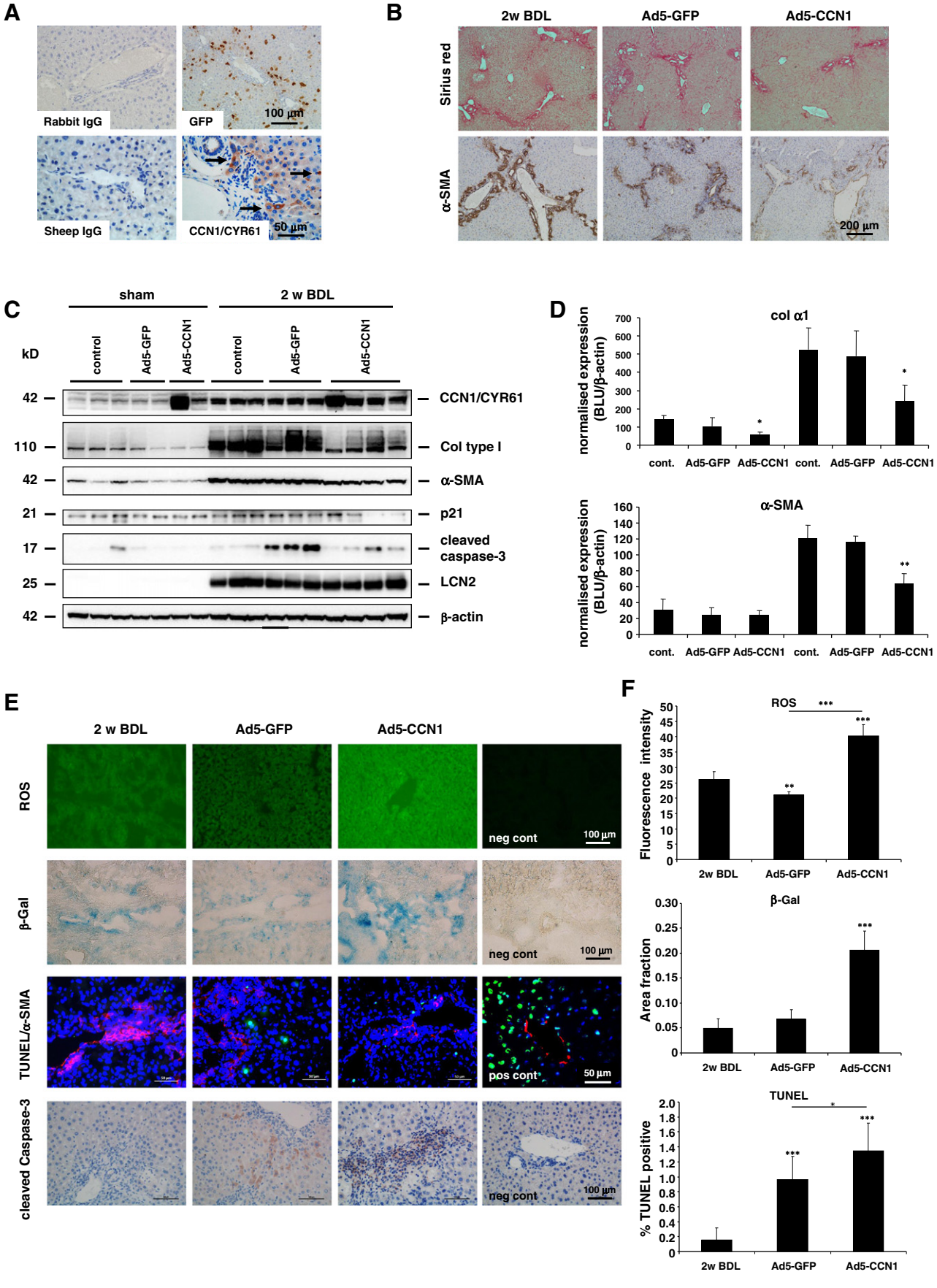
A
Rabbit IgG
GFP
100 µm
Sheep IgG
CCN1/CYR61
50 µm
B
2w BDL
Ad5-GFP
Ad5-CCN1
Sirius red
α-SMA
200 µm
C
sham
2 w BDL
control
Ad5-GFP
Ad5-CCN1
kD
42
CCN1/CYR61
110
Col type I
α-SMA
21
p21
17
cleaved caspase-3
25
LCN2
β-actin
D
col α1
normalised expression (BLU/β-actin)
cont.
Ad5-GFP
Ad5-CCN1
α-SMA
E
2 w BDL
Ad5-GFP
Ad5-CCN1
ROS
β-Gal
TUNEL/α-SMA
cleaved Caspase-3
neg cont
pos cont
100 µm
50 µm
F
ROS
Fluorescence intensity
β-Gal
Area fraction
TUNEL
% TUNEL positive
2w BDL
Ad5-GFP
Ad5-CCN1

fibrotic molecular switch that converts ECM-producing MFB into ECM-degrading senescent cells, thus imposing a self-limiting control on fibrogenesis during wound healing [4,6].

During BDL-induced hepatic fibrosis, fibroblasts within the portal tracts become activated, proliferate and express α-SMA, suggesting that they are involved in the deposition of ECM components in cholestatic fibrosis [26]. These MFB populations are distinct from HSC as verified by marker gene expression analysis [29,17,18], as they specifically express fibulin-2 and elastin. The majority of MFB in fibrotic regions were found to be desmin negative and derived from portal mesenchymal cells rather than HSC [30], the reason why we did choose pMF as an *in vitro* cellular model for anti-fibrotic effects of CCN1/CYR61. We isolated primary portal fibroblast and tested the anti-fibrotic function of CCN1/CYR61 in cultured pMF by using Ad5-CMV-CCN1 and found overexpression of CCN1/CYR61 to inhibit col1α1 and α-SMA production (*cf.* Fig. 3A–C). Inhibition of col1α1 was more prominent than α-SMA at protein levels as shown by Western blot and immunohistochemistry. Although Ad5-CMV-CCN1 significantly inhibited α-SMA mRNA production, protein expression was reduced only modestly, which might be due to the long half-life of this protein [31] and the huge amounts of α-SMA present in fully differentiated pMF. By contrast, during early periods of pMF culturing, immunohistochemistry clearly showed CCN1/CYR61 over-expression to be sufficient to attenuate α-SMA production (Fig. 3D). These findings confirmed the anti-fibrotic properties of CCN1/CYR61 overexpression through Ad5-CMV-CCN1 transduction.

CCN1/CYR61 induces fibroblast senescence through an integrin-mediated mechanism, resulting in the expression of anti-fibrotic genes to dampen fibrosis in cutaneous wound healing [4,6]. Adenoviral overexpressed CCN1/CYR61 induced pMF apoptosis instead, as evidenced by increased levels of cleaved caspase 3 (Fig. 4), the major effector caspase in apoptosis, and positive TUNEL staining. Previous reports claim CCN1/CYR61 to induce fibroblast apoptosis through its adhesion receptor integrin $\alpha_6\beta_1$ and the heparan sulfate proteoglycan, thus triggering transcription-independent p53 activation of Bax to render cytochrome c release and activation of caspase-9 and -3 [32]. We could demonstrate that CCN1/CYR61 overexpression in cultured pMF resulted in increased amounts of cleaved caspase-9 and -3 (Fig. 4A). The caspase activity showed all caspases to increase, but caspase-9 and caspases 3–7 are more prominent than caspase-8 (Fig. 4B).

We further found cultured passage pMF to acquire a general cellular senescence as shown by β-galactosidase positive staining in normal cultures, whereas Ad5-CMV-CCN1-infected cells showed both positive β-galactosidase and cellular detachment from the cell culture dishes (Fig. 5C), indicating that Ad5-CMV-CCN1 additionally induced pMF apoptosis. Protein p21 is a cyclin-dependent kinase inhibitor, which is important in cellular response to genotoxic stress and a major transcriptional target of p53 protein. In the nucleus it binds to and inhibits the activity of cyclin dependent kinases Cdk1 and Cdk2 and blocks the transition from G_1 phase into S phase or from G_2 phase into mitosis after DNA damage, thus enabling repair of damaged DNA [32]. Protein p21 is further considered as an important protein for induction of replication senescence as well as stress-induced premature senescence. We found p53 activation and increased p21 levels in pMF incubated with CCN1-Fc protein (Fig. 6C) but only slight increases in Ad5-CMV-CCN1 transduced cells. Immunocytochemistry, however, showed p21 nuclear localization in these cells (Fig. 5D), indicating that CCN1 most likely enhances pMF senescence through p53 and p21 pathways. In cytoplasm, p21 exerts anti-apoptotic effects with the ability to bind to and inhibit caspase 3, as well as the apoptotic kinases ASK1 and JNK [33]. The function of p21 in response to DNA damage probably depends on the extent of the damage. In low-level DNA damage cases such as those induced by incubation with the CCN1 protein, expression of p21 is increased. It induces cell cycle arrest, and performs anti-apoptotic activities (Fig. 6B). However, upon extensive DNA damage the amount of p21 protein decreases and the cells undergo apoptosis (Figs. 4 and 5B). This dual functionality of p21 may explain the simultaneous occurrence of senescence and apoptosis in cultured cells and whole livers after transduction of Ad5-CMV-CCN1.

It has been established that CCN1/CYR61 in ECM enables TNF-α to induce apoptosis without NFκB signaling inhibition [34,35]. We found that NFκB (pp65) activation is a compensatory cell survival response during CCN1/CYR61-induced pMF apoptosis (Fig. 4A). Overexpression of CCN1/CYR61-induced apoptosis is also seen in primary HSC and in the immortalized hepatic stellate cell line CFSC (Fig. A2A and B) suggesting that it is a general attribute of CCN1/CYR61 in profibrogenic liver cells. Additionally, CCN1/CYR61-induced ROS formation is required for CCN1/TNF-α-induced apoptosis through activation of p53 and p38 MAPK, that mediate enhanced cytochrome c release to amplify the cytotoxicity of TNF-α [36]. Our experiments showed Ad5-CMV-CCN1 infection to markedly induce ROS production that inhibits MAPK phosphatase activity resulting in p38 hyperactivation (Fig. 5B), enhancement of mitochondrial cytochrome c release, activation of initial procaspase-9, and activation of the effector caspase 3 (Fig. 4A and B). In contrast to the context-dependent role of p38, JNK activation appears generally necessary for TNF-α-induced apoptosis [37]. JNK activation was clearly evidenced in pMF infected with Ad5-CMV-CCN1.

CCN1/CYR61 was strongly expressed at the sites of inflammation, injury repair and tissue remodeling and can synergize with FasL and significantly enhance FasL-induced apoptosis in fibroblast. CCN1/CYR61 mechanically engages with integrin $\alpha_6\beta_1$ and cell surface heparan sulfate proteoglycan, leading to the ROS-dependent hyperactivation of p38 MAPK in the presence of FasL [38]. We found Ad5-CMV-CCN1-infection to specifically induce ROS formation, p38 phosphorylation and upregulation of Fas in pMF (*cf.* Figs. 4A, 5A and B), a phenomenon also observed in hepatocytes transduced with Ad5-CMV-CCN2/CTGF and Ad5-CMV-CCN3/NOV [39], suggesting that CCN proteins are critically involved in the excessive formation of free radicals and control of associated downstream cellular signaling pathways.

Compared to Ad5-CMV-CCN1 or CCN1 plasmid transfection, CCN1-Fc protein and Ad5-CMV-CCN1 conditioned media showed some degree of cellular stress as evidenced by increased LCN2 production, but pMF were driven into cellular senescence rather than apoptosis. Depending on the CCN1 protein dosage, the conditioned media contained higher levels of CCN1 resulting in some degree of cellular apoptosis.

Suppression of collagen type I production from CCN1 was shown in both Ad5-CMV-CCN1 and CCN1 protein. The CCN protein family is known to moderate the growth factors and cytokine signaling [40] and we found CCN1 to attenuate TGF-β signaling through scavenging TGF-β ligand. Ad5-CMV-CCN1 transduction in our *in vivo* BDL model did

Fig. 8. Ad5-CMV-CCN1 attenuated liver fibrosis in a BDL model. (A) Immunohistochemistry of GFP and CCN1/CYR61 showed Ad5-CMV-GFP and Ad5-CMV-CCN1 treated livers to transduce both parenchymal (hepatocytes) and non-parenchymal cells. In this analysis antibody AF 4055 (R&D Systems) was used for CCN1/CYR61 detection. (B) Sirius red and α-SMA IHC of the representative BDL livers showed Ad5-CMV-CCN1 to reduce Sirius red staining and α-SMA compared to controls. (C) Western blots of 2-week sham-operated and BDL liver lysates reflecting CCN1 upregulation in BDL liver, but Ad5-CMV-CCN1 treated livers showing higher levels of CCN1 resulting in significant diminished collagen type I and α-SMA levels, while Ad5-CMV-GFP and Ad5-CMV-CCN1 treated animals showed increased caspase-3. LCN2, the marker of liver injury was increased markedly in BDL livers, while β-actin served as loading control. (D) Collagen type I and α-SMA were quantified using Boehringer Light Unit (BLU) from Lumi-Analyst Image Analysis Software (Roche Diagnostics) normalized to β-actin. (E) Increased concentrations of ROS (*panel 1*) and elevated levels of β-Gal activity around periportal areas (*panel 2*) were found in livers that were transduced with Ad5-CMV-CCN1. In the negative control stains, the substrate was omitted. TUNEL and α-SMA co-staining (*panel 3*) showed positive areas in both Ad5-CMV-GFP and Ad5-CMV-CCN1 infected livers. However, in Ad5-CMV-CCN1 infected livers, TUNEL positive cells were limited to non-parenchymal cells around portal tracts, while in Ad5-CMV-GFP infected livers the parenchymal areas were more pronounced stained. While, the immunohistochemistry of cleaved caspase 3 (*panel 4*) revealed a positive stain in hepatocytes in Ad5-CMV-GFP transduced livers, Ad5-CMV-CCN1 infected livers showed a more positive stain in non-parenchymal cells. (F) Quantification of ROS signals, β-Gal stain, and TUNEL staining in sections taken from (E).

transduce both parenchymal and non-parenchymal liver cells, but liver cell apoptosis was mainly found in periportal areas, in line with previous reporting that in bile duct ligation models, myofibroblasts derived from portal fibroblast disappear during the resolution period by apoptosis [41]. The attenuation of liver fibrosis from Ad5-CMV-CCN1 therefore might result from the synergistic effects of cellular senescence, apoptosis around the portal areas and diminishing TGF-β signaling.

5. Conclusions

Compared to cutaneous wound healing, CCN1/CYR61 overexpression in liver fibrogenic cells, such as pMF and HSC, promotes tissue remodeling and active prevention of liver fibrosis though cellular senescence, fibrogenic cell apoptosis and attenuation of TGF-β signaling.

Supplementary data to this article can be found online at http://dx.doi.org/10.1016/j.bbamcr.2014.01.023.

Acknowledgements

This work was supported by grants from the START project, Faculty of Medicine, RWTH-Aachen University and the Deutsche Forschungsgemeinschaft (SFB/TRR57 P13). Y.A.N. is supported by the Wilhelm-Sander Foundation for Cancer Research. The authors extend their sincere thanks to Sabine Weiskirchen, Carmen Tag, and Sibille Sauer-Lehnen for technical assistance and primary cell isolation.

References

[1] P. Bork, The modular architecture of a new family of growth regulators related to connective tissue growth factor, FEBS Lett. 327 (1993) 125–130.
[2] R. Weiskirchen, CCN proteins in normal and injured liver, Front. Biosci. 16 (2011) 1939–1961.
[3] P. Bornstein, Diversity of function is inherent in matricellular proteins: an appraisal of thrombospondin 1, J. Cell Biol. 130 (1995) 503–506.
[4] J.I. Jun, L.F. Lau, Cellular senescence controls fibrosis in wound healing, Aging 2 (2010) 627–631.
[5] J.I. Jun, L.F. Lau, The matricellular protein CCN1 induces fibroblast senescence and restricts fibrosis in cutaneous wound healing, Nat. Cell Biol. 12 (2010) 676–685.
[6] L.F. Lau, CCN1/CYR61: the very model of a modern matricellular protein, Cell. Mol. Life Sci. 68 (2011) 3149–3163.
[7] S.J. Leu, N. Chen, C.C. Chen, V. Todorovic, T. Bai, V. Juric, Y. Liu, G. Yan, S.C. Lam, L.F. Lau, Targeted mutagenesis of the angiogenic protein CCN1 (CYR61). Selective inactivation of integrin alpha6beta1-heparan sulfate proteoglycan coreceptor-mediated cellular functions, J. Biol. Chem. 279 (2004) 44177–44187.
[8] A.M. Gressner, R. Weiskirchen, Modern pathogenetic concepts of liver fibrosis suggest stellate cells and TGF-β as major players and therapeutic targets, J. Cell. Mol. Med. 10 (2006) 76–99.
[9] S.L. Friedman, Evolving challenges in hepatic fibrosis, Nat. Rev. Gastroenterol. Hepatol. 7 (2010) 425–436.
[10] V. Krizhanovsky, M. Yon, R.A. Dickins, S. Hearn, J. Simon, C. Miething, H. Yee, L. Zender, S.W. Lowe, Senescence of activated stellate cells limits liver fibrosis, Cell 134 (2008) 657–667.
[11] D. Hilfiker-Kleiner, K. Kaminski, A. Kaminska, M. Fuchs, G. Klein, E. Podewski, K. Grote, I. Kiian, K.C. Wollert, A. Hilfiker, H. Drexler, Regulation of proangiogenic factor CCN1 in cardiac muscle: impact of ischemia, pressure overload, and neurohumoral activation, Circulation 109 (2004) 2227–2233.
[12] T.M. Grzeszkiewicz, V. Lindner, N. Chen, S.C. Lam, L.F. Lau, The angiogenic factor cysteine-rich 61 (CYR61, CCN1) supports vascular smooth muscle cell adhesion and stimulates chemotaxis through integrin $\alpha_6\beta_1$ and cell surface heparan sulfate proteoglycans, Endocrinology 143 (2002) 1441–1450.
[13] M. Hadjiargyrou, W. Ahrens, C.T. Rubin, Temporal expression of the chondrogenic and angiogenic growth factor CYR61 during fracture repair, J. Bone Miner. Res. 15 (2000) 1014–1023.
[14] A.N. Athanasopoulos, D. Schneider, T. Keiper, V. Alt, U.R. Pendurthi, U.M. Liegibel, U. Sommer, P.P. Nawroth, C. Kasperk, T. Chavakis, Vascular endothelial growth factor (VEGF)-induced up-regulation of CCN1 in osteoblasts mediates proangiogenic activities in endothelial cells and promotes fracture healing, J. Biol. Chem. 282 (2007) 26746–26753.
[15] K. Sawai, M. Mukoyama, K. Mori, M. Kasahara, M. Koshikawa, H. Yokoi, T. Yoshioka, Y. Ogawa, A. Sugawara, H. Nishiyama, S. Yamada, T. Kuwahara, M.A. Saleem, K. Shiota, O. Ogawa, M. Miyazato, K. Kangawa, K. Nakao, Expression of CCN1 (CYR61) in developing, normal, and diseased human kidney, Am. J. Physiol. Renal Physiol. 293 (2007) F1363–F1372.
[16] E.A. Kruglov, D. Jain, J.A. Dranoff, Isolation of primary rat liver fibroblasts, J. Investig. Med. 50 (2002) 179–184.
[17] S.K. Meurer, L. Tihaa, E. Borkham-Kamphorst, R. Weiskirchen, Expression and functional analysis of endoglin in isolated liver cells and its involvement in fibrogenic Smad signalling, Cell. Signal. 23 (2011) 683–699.
[18] Z. Li, J.A. Dranoff, E.P. Chan, M. Uemura, J. Sévigny, R.G. Wells, Transforming growth factor-β and substrate stiffness regulate portal fibroblast activation in culture, Hepatology 46 (2007) 1246–1256.
[19] S. Schäfer, O. Zerbe, A.M. Gressner, The synthesis of proteoglycans in fat-storing cells of rat liver, Hepatology 7 (1987) 680–687.
[20] H. Fehrenbach, R. Weiskirchen, M. Kasper, A.M. Gressner, Upregulated expression of the receptor for advanced glycation end products in cultured rat hepatic stellate cells during transdifferentiation to myofibroblasts, Hepatology 34 (2001) 943–952.
[21] M. Rojkind, P.M. Novikoff, P. Greenwel, J. Rubin, L. Rojas-Valencia, A.C. de Carvalho, R. Stockert, D. Spray, E.L. Hertzberg, A.W. Wolkoff, Characterization and functional studies on rat liver fat-storing cell line and freshly isolated hepatocyte coculture system, Am. J. Pathol. 146 (1995) 1508–1520.
[22] R. Weiskirchen, K. Bister, Suppression in transformed avian fibroblasts of a gene (*crp*) encoding a cysteine-rich protein containing LIM domains, Oncogene 8 (1993) 2317–2324.
[23] M. Arias, S. Sauer-Lehnen, J. Treptau, N. Janoschek, I. Theuerkauf, R. Buettner, A.M. Gressner, R. Weiskirchen, Adenoviral expression of a transforming growth factor-β1 antisense mRNA is effective in preventing liver fibrosis in bile-duct ligated rats, BMC Gastroenterol. 3 (2003) 29.
[24] E. Borkham-Kamphorst, E. Kovalenko, C.R. van Roeyen, N. Gassler, M. Bomble, T. Ostendorf, J. Floege, A.M. Gressner, R. Weiskirchen, Platelet-derived growth factor isoform expression in carbon tetrachloride-induced chronic liver injury, Lab. Invest. 88 (2008) 1090–1100.
[25] E. Borkham-Kamphorst, J. Herrmann, D. Stoll, J. Treptau, A.M. Gressner, R. Weiskirchen, Dominant-negative soluble PDGF-beta receptor inhibits hepatic stellate cell activation and attenuates liver fibrosis, Lab Invest. 84 (2004) 766–777.
[26] B. Tuchweber, A. Desmoulière, M.L. Bochaton-Piallat, L. Rubbia-Brandt, G. Gabbiani, Proliferation and phenotypic modulation of portal fibroblasts in the early stages of cholestatic fibrosis in the rat, Lab. Invest. 74 (1996) 265–278.
[27] N. Kinnman, C. Housset, Peribiliary myofibroblasts in biliary type liver fibrosis, Front. Biosci. 7 (2002) d496–d503.
[28] K.H. Kim, C.C. Chen, R.I. Monzon, L.F. Lau, Matricellular protein CCN1 promotes regression of liver fibrosis through induction of cellular senescence in hepatic myofibroblasts, Mol. Cell. Biol. 33 (2013) 2078–2090.
[29] T. Knittel, D. Kobold, B. Saile, A. Grundmann, K. Neubauer, F. Piscaglia, G. Ramadori, Rat liver myofibroblasts and hepatic stellate cells: different cell populations of the fibroblast lineage with fibrogenic potential, Gastroenterology 117 (1999) 1205–1221.
[30] M. Beaussier, D. Wendum, E. Schiffer, S. Dumont, C. Rey, A. Lienhart, C. Housset, Prominent contribution of portal mesenchymal cells to liver fibrosis in ischemic and obstructive cholestatic injuries, Lab. Invest. 87 (2007) 292–303.
[31] N.M. Sawtell, J.L. Lessard, Cellular distribution of smooth muscle actins during mammalian embryogenesis: expression of the alpha-vascular but not the gamma-enteric isoform in differentiating striated myocytes, J. Cell Biol. 109 (1989) 2929–2937.
[32] V. Todorovic, C.C. Chen, N. Hay, L.F. Lau, The matrix protein CCN1 (CYR61) induces apoptosis in fibroblasts, J. Cell Biol. 171 (2005) 559–568.
[33] J. Cmielová, M. Rezáčová, p21Cip1/Waf1 protein and its function based on a subcellular localization [corrected], J. Cell. Biochem. 112 (2011) 3502–3506(Erratum in: J. Cell. Biochem. 113 (2012) 1450).
[34] C.C. Chen, J.L. Young, R.I. Monzon, N. Chen, V. Todorović, L.F. Lau, Cytotoxicity of TNFα is regulated by integrin-mediated matrix signaling, EMBO J. 26 (2007) 1257–1267.
[35] C.C. Chen, L.F. Lau, Deadly liaisons: fatal attraction between CCN matricellular proteins and the tumor necrosis factor family of cytokines, J. Cell Commun. Signal. 4 (2010) 63–69.
[36] V. Juric, C.C. Chen, L.F. Lau, TNFα-induced apoptosis enabled by CCN1/CYR61: pathways of reactive oxygen species generation and cytochrome c release, PLoS One 7 (2012) e31303.
[37] H. Kamata, S. Honda, S. Maeda, L. Chang, H. Hirata, M. Karin, Reactive oxygen species promote TNFα-induced death and sustained JNK activation by inhibiting MAP kinase phosphatases, Cell 120 (2005) 649–661.
[38] V. Juric, C.C. Chen, L.F. Lau, Fas-mediated apoptosis is regulated by the extracellular matrix protein CCN1 (CYR61) *in vitro* and *in vivo*, Mol. Cell. Biol. 29 (2009) 3266–3279.
[39] E. Borkham-Kamphorst, S. Huss, E. Van de Leur, U. Haas, R. Weiskirchen, Adenoviral CCN3/NOV gene transfer fails to mitigate liver fibrosis in an experimental bile duct ligation model because of hepatocyte apoptosis, Liver Int. 32 (2012) 1342–1353.
[40] A. Leask, D.J. Abraham, All in the CCN family: essential matricellular signaling modulators emerge from the bunker, J. Cell Sci. 119 (2006) 4803–4810.
[41] C. Guyot, C. Combe, C. Balabaud, P. Bioulac-Sage, A. Desmoulière, Fibrogenic cell fate during fibrotic tissue remodelling observed in rat and human cultured liver slices, J. Hepatol. 46 (2007) 142–150.